Electric conductance of highly selective nanochannels

Ory Schnitzer and Ehud Yariv
Department of Mathematics, Technion — Israel Institute of Technology, Technion City 32000, Israel
(Received 20 February 2013; published 9 May 2013)

We consider electric conductance through a narrow nanochannel in the thick-double-layer limit, where the space-charge Debye layers adjacent to the channel walls overlap. At moderate surface-charge densities the electrolyte solution filling the channel comprises mainly of counterions. This allows to derive an analytic closed-form approximation for the channel conductance, independent of the salt concentration in the channel reservoirs. The derived expression consists of two terms. The first, representing electromigratory transport, is independent of the channel depth. The second, representing convective transport, depends upon it weakly.

DOI: 10.1103/PhysRevE.87.054301 PACS number(s): 66.10.Ed, 82.39.Wj, 82.45.Gj, 87.16.Vy

Nanochannels and nanopores of well-defined geometries, made possible through use of conventional fabrication methods [1], constitute key elements in nanoscale devices [2–4], with potential applications including energy conversion [5], nanofluidic transistors [6–8] and diodes [9–13], DNA translocation [14–16], and molecular sieving [17,18].

A conceptual model problem, schematically portrayed in Fig. 1, consists of a channel (length L^*, depth $2h^*$, width w^*), transversely bounded by uniformly charged walls (surface-charge density $-\sigma^*$). The channel is connected at its ends to two large reservoirs filled with a symmetric z–z electrolyte solution, where the cation and anion concentrations are equal, say c^*. Application of a voltage V^* between the reservoirs results in an ionic current I^*. The property of practical interest is the channel conductance I^*/E^*, with $E^* = V^*/L^*$ being the "applied field" magnitude. When considering "deep" channels, with h^* on the micron scale and above, electric conduction is essentially carried out through ionic electromigration, the resulting current thus being proportional to both c^* and h^*. In view of electroneutrality which prevails throughout the majority of the channel cross section, charge convection is then confined to the narrow diffuse-charge layers.

In a landmark nanochannel experiment, Stein *et al.* [19] demonstrated that the linear scaling with c^* breaks down at low salt concentration, where the conductance actually saturates at a c^*-independent value that depends only weakly upon h^*. Stein *et al.* [19] explained that the breakdown of Ohmic conductance is due to the dominance of electrokinetic effects at low salt concentrations, where the Debye width is thick enough for the diffuse-charge Debye layers formed about the "top" and "bottom" channel walls to overlap.

In the experiments of Stein *et al.* [19] the channel is several millimeters long and 50 μm wide, while its depth $2h^*$ ranges roughly between 100 nm and one micron. These figures suggest the use of a simplified electrokinetic model, where the first scale disparity ($L^* \gg w^*$) allows to approximate the transport process as being "fully developed," while the second scale disparity ($w^* \gg h^*$) allows for a two-dimensional description of the cross-sectional transport. Such a model was used by Stein *et al.* [19], assuming a monovalent solution ($z = 1$) for simplicity. The exact solution of their one-dimensional Poisson-Boltzmann equation, expressed in terms of Jacobi elliptic functions [20], provides a set of transcendental equations from which the channel conductivity can be calculated numerically. The resulting values indeed reveals the observed transition from a linear variation at high salt concentrations to a saturation at low concentrations. Using the surface-charge density as a fitting parameter, Stein *et al.* [19] obtained values of order 100 mC m^{-2}, comparable to those measured by charge titration.

We here propose using a thick-double-layer approximation to derive a closed-form approximation for the channel conductance at low salt concentrations. In this limit, and for moderate surface-charge-density values, the nanochannel consists mainly of counterions and therefore acts as a highly-selective membrane. This scenario lends itself to well-known analytic approximations, going back to the Derjaguin-Landau-Verwey-Overbeek (DLVO) theory for suspension stability [21]. Similar approximations, making use of the dominance of counterions, were used in recent years in the analysis of such problems as the anion-depleted cathodic Debye charge in overlimiting currents [22–24] and of surface conduction through the "Dukhin layer" surrounding highly-charged solid surfaces [25,26]. In the present problem, our model provides a closed-form approximation for the channel conductance which is independent of c^* and weakly depends upon h^*.

We employ a rather standard dimensionless notation, normalizing length variables by h^*, the electric potential by the thermal voltage $\varphi^* = k^*T^*/ze^*$ (in which k^* is Boltzmann's constant, T^* the thermodynamic temperature, and e^* the proton charge), and the ionic concentrations by c^*. Ionic fluxes are normalized by the diffusive scale D^*c^*/h^*, wherein D^* is the cationic diffusivity. The velocity field is normalized by the Maxwell scale $\epsilon^*\varphi^{*2}/\mu^*h^*$, wherein ϵ^* and μ^* are the dielectric permittivity and Newtonian viscosity of the electrolyte solution.

The essentially two-dimensional transport is described using a Cartesian xy-coordinate system (see Fig. 1), the x-axis pointing along the channel direction and the y-axis lying perpendicular to the bounding walls (at $y = \pm 1$). We seek a fully developed distribution, where the ionic concentrations $c^{\pm}$ and the longitudinal velocity u are independent of x. Because of the continuity equation and impermeability to fluid at the bounding walls there is no fluid motion in the y-direction. Moreover, we also postulate a fully-developed electric field, where the electric potential adopts the form (resembling the

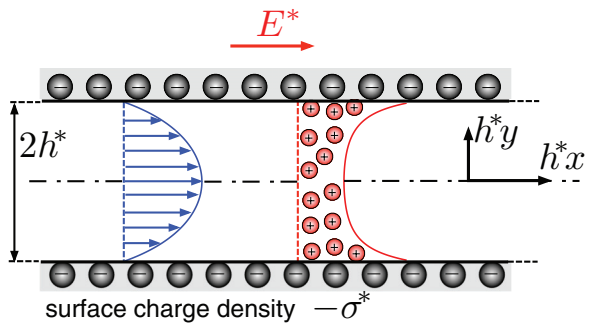

FIG. 1. (Color online) Nanochannel schematic. The shapes of the counterion-concentration distribution (red) and electrokinetic-flow profile (blue), respectively, correspond to expressions (13) and (17), evaluated for $\sigma = 5$.

pressure field in unidirectional pressure-driven flows)

$$-Ex + \varphi(y), \tag{1}$$

where $E = h^* E^*/\varphi^*$ is the dimensionless applied field. The Nernst-Planck conservation equations in the x-direction are then identically satisfied, while those in the y-direction imply uniform ionic fluxes; in view of ionic impermeability at the inert channel walls $y = \pm 1$, both of these fluxes must actually vanish:

$$-\frac{dc^{\pm}}{dy} \mp c^{\pm}\frac{d\varphi}{dy} = 0. \tag{2}$$

The ionic concentration are accordingly Boltzmann distributed,

$$c^{\pm} = A^{\pm} e^{\mp\varphi}, \tag{3}$$

where $A^{\pm}$ are constants. Substitution into Poisson's equation yields the nonlinear differential equations

$$\frac{d^2\varphi}{dy^2} = \frac{1}{2}h^2(A^- e^{\varphi} - A^+ e^{-\varphi}). \tag{4}$$

Here,

$$h = h^*\kappa^* \tag{5}$$

is the ratio of of the semidepth h^* to the Debye width $1/\kappa^*$, defined by

$$\kappa^{*2} = \frac{2ze^*c^*}{\epsilon^*\varphi^*}. \tag{6}$$

The second-order equation (4) is supplemented by the Gauss-type boundary conditions

$$\frac{d\varphi}{dy} = \mp\sigma \quad \text{at} \quad y = \pm 1, \tag{7}$$

where σ is the ratio of σ^* to $\epsilon^*\varphi^*/h^*$. With no loss of generality, the surface-charge density $-\sigma^*$ is assumed negative (as in most solid-electrolyte interfaces), whereby $\sigma > 0$.

It is a common practice in electrokinetic analyses of nanochannels to assume a Boltzmann distribution which reduces to the reference concentration at zero potential (as in Ref. [19]); in the present notation, this would correspond to setting $A^{\pm} = 1$ (whereby Eq. (4) becomes the familiar Poisson-Boltzmann equations, cf. Eq. (1) in Ref. [19]). This procedure is standard in thin-double-layer analyses, where it represents asymptotic matching between the Debye scale and the bulk [27]. In analyzing nanochannels, however, where the double layers overlap, this procedure is unwarranted. As the fully developed concentration profiles cannot be directly matched to the uniform concentrations in the reservoirs, there is no way to determine $A^{\pm}$ within the fully developed framework. We accordingly proceed without making any *a priori* assumptions that these constants are identical (let alone equal to unity).

We now consider the thick-double-layer limit

$$h \ll 1 \tag{8}$$

while $\sigma \sim O(1)$. Naively, Eq. (4) may appear to suggest the expansion $\varphi(y;h) \approx \phi(y) + O(h^2)$; however, the resulting leading-order equation, $d^2\phi/dy^2 = 0$, is incompatible with conditions (7). The limit (8) is a singular one, representing the dominance of counter ions throughout the entire channel cross-section. Thus, we postulate the expansion

$$\varphi(y;h) \approx 2\ln h + \phi(y) + O(h^4) \tag{9}$$

corresponding to large cation concentration [see Eq. (3)]. At leading order, Eq. (4) then yields

$$\frac{d^2\phi}{dy^2} = -\frac{1}{2}A^+ e^{-\phi}. \tag{10}$$

The solution of this cation-dominated balance, possessing the requisite transverse symmetry, is

$$\phi = \ln\frac{A^+\cos^2 py}{4p^2}, \tag{11}$$

where with no loss of generality $p > 0$ [28]. Conditions (7) yield the one-to-one correspondence

$$p\tan p = \frac{\sigma}{2} \tag{12}$$

between p and σ. Remarkably, the cationic concentration, obtained from Eq. (3), is independent of A^+,

$$c^+ \approx \frac{4h^{-2}p^2}{\cos^2 py}. \tag{13}$$

Note the h^{-2} scaling, representing the intensification of counterions. Clearly, the co-ion concentration is $O(h^2)$. Thus, the conduit effectively constitutes a highly selective single-pore membrane.

With the electric potential known, the longitudinal velocity u is obtained from the Stokes equation in the x-direction,

$$\frac{d^2u}{dy^2} = E\frac{d^2\varphi}{dy^2}. \tag{14}$$

Two successive integrations in conjunction with the no-slip conditions

$$u = 0 \quad \text{at} \quad y = \pm 1, \tag{15}$$

yield the velocity profile

$$u \approx E\{\phi(y) - \phi(1)\}. \tag{16}$$

Substitution of Eq. (11) reveals that it, too, is independent of A^+:

$$u \approx E \ln \frac{\cos^2 py}{\cos^2 p}. \tag{17}$$

In the present fully developed model, the cationic flux j in the x-direction consists of electromigratory and convective contributions, both proportional to c^+:

$$j \approx \{E + \alpha u(y)\} c^+(y). \tag{18}$$

Here, $\alpha = \epsilon^* \varphi^{*2}/\mu^* D^*$ is the cationic ion-drag coefficient, $\lesssim 0.5$ for typical ionic size [29]. We therefore proceed assuming

$$\alpha \sim O(1). \tag{19}$$

Thus, the cationic flux is $O(h^{-2})$, while the comparable anions flux is $O(h^2)$, negligibly small. Specifically, substitution of Eqs. (13) and (17) yields

$$j \approx \frac{4Eh^{-2}p^2}{\cos^2 py} \left(1 + \alpha \ln \frac{\cos^2 py}{\cos^2 p}\right). \tag{20}$$

In view of the effective absence of anions at leading order, j also constitutes the *electric-current* density, normalized by $ze^* D^* c^*/h^*$. The total current through the conduit, normalized by $ze^* D^* c^* w^*$, is readily obtained via integration over y, yielding $4h^{-2}E\sigma(1 + 2\alpha - 4\alpha p^2/\sigma)$. The channel conductance—the ratio of the corresponding dimensional current I^* to the dimensional field magnitude E^*—is then readily obtained. Making use of Eq. (6) we find

$$\text{conductance} = \frac{2\sigma^* D^* w^*}{\varphi^*}(1 + 2\alpha - 4\alpha p^2/\sigma). \tag{21}$$

Expression (21) is the main result of this report. Note that it is independent of c^*. It is affected however by the channel semidepth h^* through its dependence (both directly, as well as indirectly through p) upon $\sigma = \sigma^* h^*/\epsilon^* \varphi^*$. Note that α is independent of both c^* and h^*. At small σ [but still $\gg h$, see Eq. (23)] it follows from Eq. (12) that $p^2 \to \sigma/2$, whereby the dimensionless conductance, normalized by $2\sigma^* D^* w^*/\varphi^*$, approaches unity. At large σ Eq. (12) implies $p \to \pi/2$, whereby the dimensionless conductance goes to $1 + 2\alpha$, or, in dimensional notation,

$$\text{conductance} \to \frac{2\sigma^* D^* w^*}{\varphi^*} \left(1 + \frac{2\epsilon^* \varphi^{*2}}{\mu^* D^*}\right). \tag{22}$$

The variation of the dimensionless conductance with σ is portrayed in Fig. 2 for $\alpha = 0.5$.

The dimensional factor $2\sigma^* D^* w^*/\varphi^*$ characterizing the conductance (21) is readily explained. In view of cross-sectional electroneutality, the surface-charge density $-\sigma^*$ at the two bounding wall implies an average volume-charge density σ^*/h^*. This is true, of course, regardless of the Debye width. In the present limit (8) of thick double layer, this density is attributed to cations, implying an average *ionic* concentration $\sigma^*/ze^* h^*$. Since the electric field in the x-direction is transversely uniform (with magnitude E^*), this average concentration gives rise through electromigration to an average cationic flux provided by product of that concentration, the cations charge ze^* and mobility $D^*/k^* T^*$,

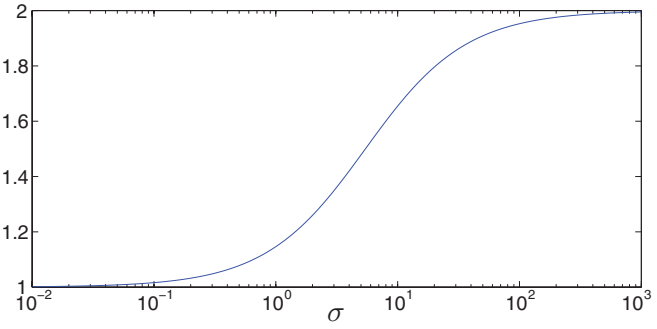

FIG. 2. (Color online) The dimensionless channel conductance, calculated using Eqs. (12) and (21), as a function of $\sigma = \sigma^* h^*/\epsilon^* \varphi^*$, for $\alpha = 0.5$.

and E^*. The corresponding current density is obtained by multiplying by the cation charge ze^* and cross-sectional area $h^* w^*$. This results in the h^*-independent conductance $2\sigma^* D^* w^*/\varphi^*$, corresponding to the electromigratory term in expression (21). Because of the attendant electrokinetic flow, the conductance is also affected by a convective term, proportional to α. This term, proportional to the *product* of c^+ and u, cannot be determined using average quantities: rather, its evaluation requires the detailed transverse distribution of these fields. In view of relation (19), this term is comparable to the electromigratory one.

It is worth noticing that the reference scale c^* eventually plays no role at the field distributions obtained using the thick-double-layer approximation, nor does it affect the channel conductance. This remarkable feature is related to the previously mentioned absence of direct linkage between the fully developed fields and the reservoir conditions. It thus appears that the only situation in which a fully developed description can be obtained for a "long" nanochannel is the thick-double-layer limit addressed herein. In all other situations, it may be that the resolution of the effective channel conductance involves matching with the reservoir conditions. In view of that observation, the validity of the electrokinetic model used by Stein *et al.* [19], where the Boltzmann distribution were *a priori* associated with the reservoir salt concentration, is dubious.

As already mentioned, the electrokinetic description of Stein *et al.* [19] can only provide the channel conductance by a numerical solution. It is accordingly less informative than the present model, which provides the closed-form expression (21). This expression is independent of the reservoir concentration, in agreement with experimental observations at low salt concentrations. Moreover, it also predicts a weak dependence upon the channel depth. Curiously, a dependence upon channel depth is evident in the experimental results of Stein *et al.* [19] (see their Fig. 2 and notice the logarithmic scale). Admittedly, these results do not correlate with the monotonic variation with h^*, as predicted in the present Fig. 2.

In their paper, Stein *et al.* [19] provide degenerate results of their electrokinetic model for low salt concentrations [see the discussion following their Eq. (6)]. Their expression for the channel conductance, which is independent of both the salt concentration *and* the channel depth, is analogous to the present large-σ limit (22). (There appears to be a factor-2 error in the convective term appearing in the expression

provided by Stein *et al*. [19].) Stein *et al*. [19] claim that their weak-concentration limit applies when (in the present notation) $\sigma^* \gg e^* c^* h^*$. This is incorrect, as can be verified from the present analysis. Using Eq. (6), it is readily verified that in dimensional notation the limit $\sigma \gg 1$ actually reads $\sigma^* \gg e^* c^* / \kappa^{*2} h^*$—a much stricter criteria.

In many electrokinetic analyses, one assumes that the natural scale for σ^* is $\epsilon^* \varphi^* \kappa^*$ [29]. In that case, again using Eq. (6), the dimensional density σ^* is of order $e^* c^* / \kappa^*$, certainly satisfying the criteria $\sigma^* \gg e^* c^* h^*$ put forward by Stein *et al*. [19]. In the present notation, however, such scaling would imply

$$\sigma \sim O(h) \ll 1. \tag{23}$$

In that limit, the present thick-double-layer limit breaks down, let alone approximation (22). It is important to emphasize that analytic progress was made possible here because of the predominance of counterions. The thick-double-layer limit $h \ll 1$ only constitutes a *necessary* condition for that to happen: indeed, it is clear that when the surface-charge density is small, there would be no significant difference between the concentrations of the two ionic species.

This work was supported by the Israel Science Foundation (Grant No. 184/12).

[1] P. Abgrall and N. T. Nguyen, Anal. Chem. **80**, 2326 (2008).
[2] J. C. T. Eijkel and A. Berg, Microfluid Nanofluid **1**, 249 (2005).
[3] R. B. Schoch, J. Han, and P. Renaud, Rev. Mod. Phys. **80**, 839 (2008).
[4] W. Sparreboom, A. Van Den Berg, and J. C. T. Eijkel, Nature Nanotech. **4**, 713 (2009).
[5] J. Yang, F. Lu, L. W. Kostiuk, and D. Y. Kwok, J. Micromech. Microeng. **13**, 963 (2003).
[6] R. Karnik, R. Fan, M. Yue, D. Li, P. Yang, and A. Majumdar, Nano Lett. **5**, 943 (2005).
[7] H. Daiguji, Y. Oka, and K. Shirono, Nano Lett. **5**, 2274 (2005).
[8] Z. Jiang and D. Stein, Phys. Rev. E **83**, 031203 (2011).
[9] Z. Siwy, I. D. Kosińska, A. Fuliński, and C. R. Martin, Phys. Rev. Lett. **94**, 048102 (2005).
[10] I. Vlassiouk and Z. S. Siwy, Nano Lett. **7**, 552 (2007).
[11] J. Cervera, B. Schiedt, and P. Ramirez, Europhys. Lett. **71**, 35 (2007).
[12] R. Karnik, C. Duan, K. Castelino, H. Daiguji, and A. Majumdar, Nano Lett. **7**, 547 (2007).
[13] Y. Yan, L. Wang, J. Xue, and H.-C. Chang, J. Chem. Phys. **138**, 044706 (2013).
[14] R. M. M. Smeets, U. F. Keyser, D. Krapf, M. Y. Wu, H. Nynke, and C. Dekker, Nano Lett. **6**, 89 (2006).
[15] D. Fologea, J. Uplinger, B. Thomas, D. S. McNabb, and J. Li, Nano Lett. **5**, 1734 (2005).
[16] V. V. Thacker, S. Ghosal, S. Hernández-Ainsa, N. A. W. Bell, and U. F. Keyser, Appl. Phys. Lett. **101**, 223704 (2012).
[17] J. Han, S. W. Turner, and H. G. Craighead, Phys. Rev. Lett. **83**, 1688 (1999).
[18] J. Han, J. Fu, and R. B. Schoch, Lab Chip **8**, 23 (2007).
[19] D. Stein, M. Kruithof, and C. Dekker, Phys. Rev. Lett. **93**, 035901 (2004).
[20] S. H. Behrens and M. Borkovec, Phys. Rev. E **60**, 7040 (1999).
[21] E. J. W. Verwey and J. T. G. Overbeek, *Theory of the Stability of Lyophobic Colloids* (Elsevier, Amsterdam, 1948).
[22] K. T. Chu and M. Z. Bazant, SIAM J. Appl. Math. **65**, 1485 (2005).
[23] E. Yariv, Phys. Rev. E **80**, 051201 (2009).
[24] E. Yariv, SIAM J. Appl. Math. **71**, 2131 (2011).
[25] O. Schnitzer and E. Yariv, Phys. Rev. E **86**, 021503 (2012).
[26] O. Schnitzer and E. Yariv, Phys. Rev. E **86**, 061506 (2012).
[27] E. Yariv, Chem. Eng. Commun. **197**, 3 (2010).
[28] Another one-parametric family of solutions, $\ln(A^+ \cosh^2 py/4p^2)$ (cf. Ref. [22]), is incompatible with conditions (7) on the *negatively* charged walls ($\sigma > 0$).
[29] D. A. Saville, Annu. Rev. Fluid Mech. **9**, 321 (1977).